Iron phthalocyanine decorated nitrogen-doped graphene biosensing platform for real-time detection of nitric oxide released from living cells

Huiying Xu, Chong Liao, Yujie Liu, Bang-Ce Ye, and Baohong Liu

Anal. Chem., **Just Accepted Manuscript** • DOI: 10.1021/acs.analchem.7b04419 • Publication Date (Web): 06 Mar 2018

Iron phthalocyanine decorated nitrogen-doped graphene biosensing platform for real-time detection of nitric oxide released from living cells

Huiying Xu,† Chong Liao,† Yujie Liu,‡ Bang-Ce Ye*† and Baohong Liu*‡

†Lab of Biosystem and Microanalysis, State Key Laboratory of Bioreactor Engineering, East China University of Science and Technology, Shanghai 200237, China

‡Department of Chemistry, Collaborative Innovation Center of Chemistry for Energy Materials and State Key Lab of Molecular Engineering of Polymers, Fudan University, Shanghai 200433, China

ABSTRACT: Nitric oxide (NO) is a transcellular messenger involved in many physiological and pathological processes, but the real-time detection of NO in biological systems is still challenging due to its rapid diffusion, low concentration and short half-life. A novel electrochemical sensing platform based on iron phthalocyanine (FePc) functionalized nitrogen-doped graphene (N-G) nanocomposites was constructed to achieve in situ monitoring of NO released from living cells on the sensing layer. By taking advantage of the synergetic effect of N-G and FePc nanocomposites, the N-G/FePc sensor displays excellent electrocatalytic activity towards NO with a high sensitivity of 0.21 $\mu A\ \mu M^{-1}\ cm^{-2}$ and a low detection limit of 180 nmol L^{-1}. The following layer-by-layer assembly of poly-L-lysine (PLL) and Nafion further improved the capacity of resisting disturbance as well as the biocompatibility of the sensing interface. The flexible design of the ITO substrate based electrode provides a more controlled cellular biosensing system which could capture molecular signals immediately after NO released from human umbilical vein endothelial cells (HUVECs). The exhibited additional features of high sensitivity, rapid response and ease of operation implies that the proposed N-G/FePc/Nafion/PLL ITO biosensor is a promising powerful platform in various complex biological systems.

Nitric oxide (NO), identified as an endothelial derived relaxation factor (EDRF),[1] is a key free-radical messenger in many biological processes, such as vasodilation, blood pressure regulation, inhibition of platelet activity, neural communication, and immune response.[2-4] These processes can be regulated by endogenous enzymatic NO production from L-arginine via a family of NO synthases (NOSs) present in various cell types due to the small size and lipophilic nature of NO which enable it to cross cell membranes and to diffuse to its biological targets.[2,5] On the other hand, the overproduction of cellular NO is related to several diseases including rheumatoid arthritis, cancer, transplant rejection, and Alzheimer's disease.[6-8] Thus, real-time quantification of NO released from living cells is in great demand concerning the fields of pathology and medicinal research.

However, real-time quantitative measurements of NO in biological systems are still a challenge due to its trace level release from cells, short half-life, rapid diffusion and oxidation by O_2. To date, a variety of analytical approaches have been used to detect NO in media such as cell cultures and tissues. The most commonly developed techniques, such as chemiluminescence method, UV-vis spectrophotometry and fluorophotometry usually require chemical time-consuming procedures for sample pre-treatment and are unavailable for *in vivo* detection.[8-11] In contrast, electrochemical sensors are particularly attractive on account of their relative simplicity and low detection limit, allowing the direct, real-time and fast measurement of NO concentration in biological samples.[12-16]

Metal (e.g., Co and Fe) phthalocyanines (MPc), as excellent electrocatalysts, have been extensively employed for electrochemical oxidation of many important analytes based on their macrocyclic nature including extended π-systems which endowed them ability to undergo fast redox processes with minimal reorganizational energies.[17-19] Electrodes modified with metallophthalocyanines have been used as electrochemical sensors in the study of the oxidation of NO.[9,11,20-21] Among them, Nyokong et al. have shown that FePc presents the highest activity for the NO oxidation except the poor stability in the sense.[22] Therefore, it is desirable to develop stable MPc-based materials to increase the sensitivity and electron transfer rates for electrochemical detection of NO. Recently, Huang et al. reported a novel NO sensor based on metalloporphyrin (phthalocyanine and salen) and 3-aminophenylboronic acid (APBA) co-functionalized reduced graphene oxide. The reversible reactivity between APBA and cell membrane carbohydrates allows practical reusability.[23]

Due to the delocalized conjugated system with the sp^2-hybridised carbon frameworks formed by the lone electron pairs of nitrogen atoms, nitrogen-doped graphene (N-G) can improve the reactivity and electrocatalytic performance of graphene (G) which is an excellent substrate with large surface area and superior electrical conductivity. Moreover, N-G provides abundant binding sites for non-covalent functionalization as well as the enhanced biocompatibility and sensitivity in biosensing applications.[24-27] The introduction of organometallic centers such as FePc to N-G may bring out novel electrocatalytic properties due to the excellent catalytic activities of

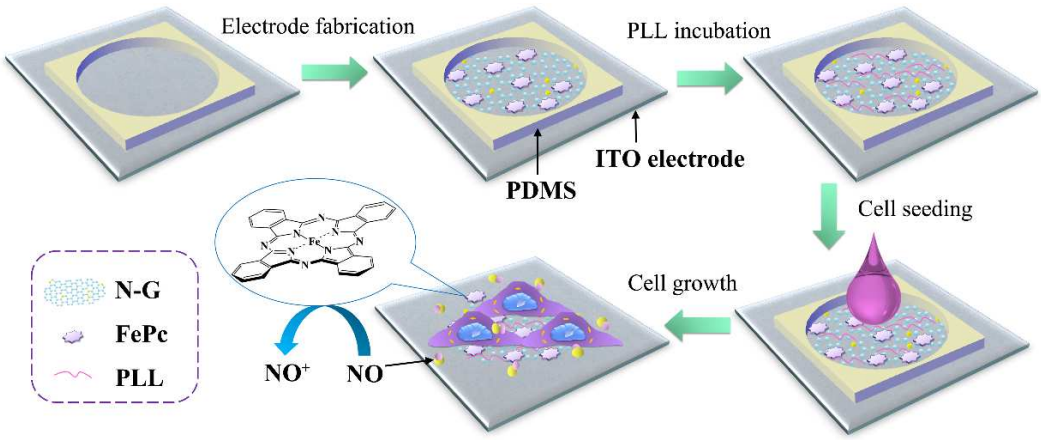

Scheme 1. Schematic illustration of the N-G/FePc/Nafion/PLL ITO electrode for real-time monitoring of NO release from living cell

both N-G and FePc. As a matrix of FePc molecules, the prominent advantage of N-G is that it could greatly facilitate the electron transfer between the electroactive species and the electrode surface of the N-G supported electrocatalysts.[28]

In this work, we developed a novel approach based on the N-G/FePc/Nafion/PLL composite modified indium tin oxide (ITO) electrode for real time electrochemical detection of nitric oxide molecule released from Human umbilical vein endothelial cells (HUVECs) under the drug stimulations (Scheme 1). The N-G was functionalized with FePc via π-π interaction,[29,30] and the resulting nanocomposites offered the ITO electrode excellent catalytic properties as a sensing platform not only served as an electrochemical sensing interface but also served as a substrate for cell growth and adhesion because of its both high electrical conductivity and optically transparent property.[31,32] After further coating with Nafion and Poly-L-lysine (PLL), this NO sensor revealed superior analytical performance towards NO and could facilitate the attachment of cells to the surface of the electrodes.[32]

EXPERIMENTAL SECTION

Chemicals and Reagents. Nitrogen doped graphene (3.0-5.0 at% nitrogen), graphene oxide (99%) (GO) and graphene were purchased from Nanjing XFNANO Materials Tech Co. (China). Fe(II)Pc, 0.01% poly-L-lysine solution, 5% Nafion, L-arginine, and NOS inhibitor Nω-nitro-L-arginine methyl ester hydrochloride (L-NAME) were purchased from Sigma Aldrich. The phosphate buffer solution (PBS) (pH 7.4) (GIBCO, Invitrogen) was used as the electrolyte throughout the whole electrochemical measurements. All other chemicals used were of analytical reagent grade, and the aqueous solutions were prepared with doubly distilled water.

Equipment. Transmission electron microscopy (TEM) measurements were performed on a JEM-2100F transmission electron microscope at 200 kV. The Ultraviolet-Visible (UV–vis) absorption spectra were recorded on an UV–vis Spectrophotometry 8453 (Agilent, USA). X-ray powder diffraction (XRD) analysis was performed on a Rigaku Rotoflex RU 200B diffractometer equipped with Cu Kα radiation (λ=1.54178 Å). Scanning electron microscopy (SEM) images were obtained using a Hitachi S-4800 filed emission scanning electron microscopy at an accelerating voltage of 1 kV. X-ray photoelectron spectroscopy (XPS) data were obtained with a PHI-5000C ESCA system (Perkin Elmer, USA) using 250 W Al Kα radiation. Electrochemical data were obtained on a CHI630E electrochemical workstation (Shanghai Chenhua Co.) at room temperature. A three-electrode system was employed, with modified ITO electrode (surface area of 0.5 cm^2) as the working electrode, a saturated calomel electrode as the reference electrode, and a platinum wire as the auxiliary electrode.

Preparation of NO in solution. NO was prepared according to reported literature procedures.[33,34] In brief, all glassware and PBS solution were deoxygenated with nitrogen gas prior to preparation. Next, NO gas was generated by using a constant pressure funnel slowly dropping 6 M H_2SO_4 into a glass flask containing saturated $NaNO_2$ solution, followed by passing the gas sequentially through 2 M NaOH solutions to remove oxygen and other nitrogen oxides. Finally, NO saturated solution was obtained by bubbling NO gas into a sealed brown bottle containing 10 mL deoxygenated phosphate buffer solution (PBS, pH 7.4) for 30 minutes. According to the literature, the saturated NO solution is 1.8 mM at 20 ^oC[33,35] and stored in the dark at 0 ^oC to ensure stability for 3 h.

Construction of N-G/FePc/Nafion/PLL ITO electrode. For the fabrication of the ITO electrode, the ITO glass substrates were purchased from South China Xiang Science & Technology Co. Ltd. (China). The resistivity of the ITO was less than 7 Ω/square, with thickness was 1.1 mm, and its transmittance was greater than 84%. Prior to modification, ITO coated glass slides were cut into 1.5 cm × 2.0 cm pieces using a diamond glass cutter, and then connected to copper wires by conductive silver paste plus (SPI, USA). Each ITO slide was sonicated sequentially in acetone, ethanol and deionized water, each for 10 min, following dried under nitrogen stream.

To prepare N-G/FePc composite, highly dispersed N-G (5 mg) in dimethylformamide (DMF) (5 mL) was successively added to a solution of FePc in DMF (1 mL, 1 mg/mL) and the resulting suspension was ultrasonically dispersed for 1 h. Above suspension of N-G/FePc (5 μL) was deposited on the cleaned ITO slide and dried at room temperature to obtain the N-G/FePc modified ITO electrode. Subsequently, a coating of Nafion was deposited by spreading 2 μL Nafion solution

(0.1%) on the substrate and air dried, to form a stable film, which could improve the adhering ability of N-G/FePc on the ITO electrode surface. For coating slides with poly-L-lysine, the ITO electrode was immersed into 0.01% (w/v) poly-L-lysine solution for a 5 min incubation and then washed thoroughly with water to remove excess solution. Similarly, the N-G/Nafion/PLL ITO electrode, FePc/Nafion/PLL ITO electrode, GO/FePc/Nafion/PLL ITO electrode and G/FePc/Nafion/PLL ITO electrode were prepared for comparison. Afterwards, the prepared ITO electrodes were stored at 4 °C before testing.

Cell culture and real time monitoring cell released NO molecules. Human umbilical vein endothelial cells (HUVECs) (ALLCELLS, Shanghai) were cultured in a humidified incubator (95% air with 5% CO_2) at 37 °C with a complete medium designed for optimal growth of endothelial cells in vitro. A 6 mm thick PDMS containing a hole (8 mm in diameter) was used as a temporary chamber to promote cell attachment and was fixed by two iron clamp on the ITO slides. The N-G/FePc/Nafion/PLL ITO slides were placed in a Petri dish with HUVECs seeded in the hole at a density of 2×10^5 cells/cm^2 and allowed to adhere for 18 h. A bare ITO electrode was used to culture cells at the same conditions for comparison. The PDMS chamber was removed slightly after 2 h when most of cells had been adherence, and then the cells were rinsed three times with PBS to remove loosely bound cells. Amperometric measurements were conducted under mildly stirred during cell released NO measurement. During amperometric test, the cells were stimulated by injecting stimulus L-Arg and L-NAME was employed as an inhibitor of nitric oxide synthetase (NOS) in control experiment.

RESULTS AND DISCUSSION

Characterization of N-G/FePc modified electrode. The surface morphology of the N-G/FePc deposited on ITO plate was examined by SEM. As shown in Figure 1A, the purified N-G has a continuous network of micron-sized individual sheets with numerous wrinkles and edges which are believed to facilitate electron transfer. When FePc is associated with N-G, FePc (seen as shiny white dots) with varying particle size from several to tens of nanometers uniformly disperse on the surfaces of N-G (Figure 1B). After this complexation process, the graphene layers change to be more densely sheets which can anchor more FePc particles. TEM image of the N-G/FePc nanocomposites in Figure S1 (supporting information) also reveals that FePc molecules are well dispersed onto the surfaces of N-G. The homogeneously distributed FePc would provide improved electrocatalytic properties to the N-G, and the resulting nanocomposites will be used as a superior substrate for the development of electrochemical sensors.

Then, UV-Vis spectroscopy was used to demonstrate the non-covalent binding of FePc on the N-G surface. UV-Vis absorption spectra of FePc in DMF showed a strong soret peaks at 330 nm and a sharp Q band at 659 nm, respectively (Figure 1C). However, the N-G/FePc nanocomposites witnessed a red-shift for the absorption band of phthalocyanine at 693 nm along with a decrease in absorption intensity. The large bathochromic shift of 34 nm in ground-state absorption is associated with conformational changes such as molecular flattening in the phthalocyanine upon π-π interaction with electrostatically charged surfaces of N-G.[15]

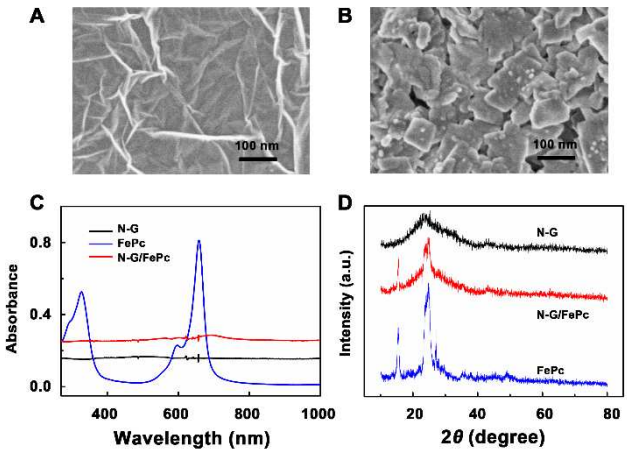

Figure 1. SEM images of (A) N-G ITO, (B) N-G/FePc ITO. (C) UV−vis spectra of N-G (black line), FePc (blue line) and N-G/FePc (red line). (D) XRD patterns of N-G, FePc and N-G/FePc.

The XRD patterns were employed to study the structure of N-G, FePc and N-G/FePc. As shown in Figure 1D, the XRD pattern of the pristine N-G powder exhibits a characteristic strong diffraction peaks at 2 θ = 23.68° (002) and a weak diffraction peak at 2 θ = 43° (100).[36] The diffraction peaks of FePc powder located at 15.5° and 24.6° correspond respectively to the lattice spacing of 5.7 and 3.6 Å.[37] As for the patterns of N-G/FePc compounds, both characteristic peaks can be observed at 2θ = 15.5° and 43° as well as the peaks centered at about 24.3°. The similar peaks to pristine FePc agree well with the status that FePc was anchored on N-G through the π–π interaction and further demonstrate the successful loading of FePc on N-G surface.[36, 37]

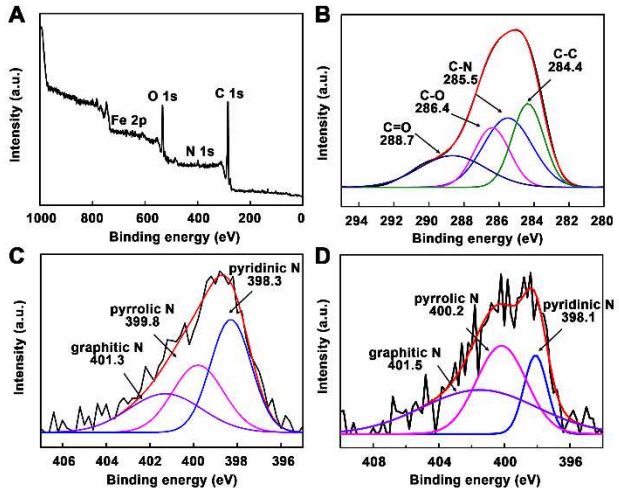

Figure 2. (A) XPS survey spectrum, (B) C 1s core level spectrum and (C) N 1s core level spectrum of N-G/FePc. (D) N 1s core level spectrum of N-G.

XPS data have also been used to characterize the chemical structure of N-G/FePc nanocomposite. As shown in the survey scan spectrum of Figure 2A, there exist four peaks centered at 285.0, 399.0, 534.6 and 710.0 eV corresponding to C 1s, N 1s, O 1s and Fe 2p, respectively, suggesting that FePc has been successfully incorporated with N-G. In the C 1s core-line

spectra of N-G/FePc (Figure 2B), the main peak is fitted with four peaks at 284.4 (C–C), 285.5 (C–N), 286.4 (C–O) and 288.7 eV (C=O), respectively. Similarly, N 1s peak can be fitted into three components (Figure 2C). The intense peaks located at 398.3 eV and 399.8 eV are assigned to nitrogen atoms with "pyridinic" and "pyrrolic" chemical structures, which can contribute to the π-conjugated system with a pair of p-electrons in the graphene layers and the high energy peak at 401.3 eV is commonly attributed to graphitic nitrogen.[24,38-40] In addition, the same peaks were also observed for N-G at binding energies of 398.1 eV for pyridinic nitrogen, 400.2 eV for pyrrolic nitrogen, and 401.5 eV for graphitic nitrogen (Figure 2D). The slight shift of binding energy suggests the π-π interaction and synergetic effect between N-G and FePc. As a result, the nanocomposites have been successfully formed and retain the electronic properties of N-G.

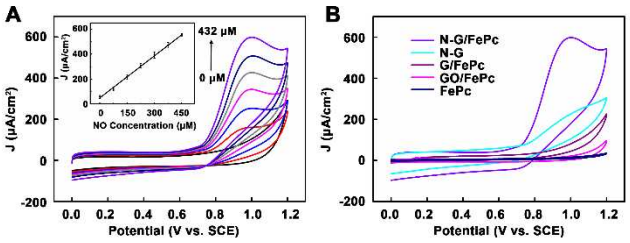

Figure 3. (A) CV of N-G/FePc/Nafion/PLL ITO electrode in 0.01 M PBS (pH 7.4) containing various concentrations of NO (0, 72, 144, 216, 288, 360, 432 μM). (B) CV of five different materials modified ITO electrode in 0.01 M PBS (pH 7.4) containing 432 μM NO.

Electrocatalytic oxidation of NO at the N-G/FePc/Nafion/PLL ITO electrode. The electrochemical response of the microsensors to NO was evaluated by cyclic voltammetry (CV) following successive additions of a saturated NO solution to the PBS electrolyte with a scan rate of 100 mV s^{-1}. In the absence of NO, only the typical capacitive behavior caused by its double layer over the entire potential (0.0 to 1.2 V vs. SCE) was observed (Figure 3A, green curve). Upon the addition of various amount of NO into solution, the voltammetric behavior of the N-G/FePc/Nafion/PLL ITO sensor changed dramatically, with an obvious catalytic oxidation peak located at 0.85 V (Figure 3A). As expected, the anodic peak currents increased by an equal proportion with the increase of NO concentrations and showed a clear linear correlation in anodic peak currents with respect to the increase in NO concentrations and the linear correlation coefficient of 0.998 (Figure 3A, inset), indicating that the modified electrode can be used as a biosensor for quantitative detection of NO. The excellent electrocatalytic activity of N-G/FePc/Nafion/PLL ITO electrode could be considered to result from the combination of the catalytic activities of FePc and N-G, where more active sites for the catalytic redox action were induced by the high density and well-distributed FePc on the surface of N-G.

Differences in the electrochemical behaviour of various electrodes (a) N-G/FePc/Nafion/PLL ITO, (b) N-G/Nafion/PLL ITO, (c) FePc/Nafion/PLL ITO, (d) GO/FePc/Nafion/PLL ITO and (e) G/FePc/Nafion/PLL ITO for the oxidation of NO were examined via CV with a scan rate of 100 mV s^{-1} (Figure 3B). When NO was added in the solution, the oxidation current of FePc/Nafion/PLL ITO electrode increased very slightly. Similar response was also observed at GO/FePc/Nafion/PLL ITO electrode due to the poorer conductivity of GO than that of N-G on the electrodes. The response of G/FePc/Nafion/PLL ITO electrode was also much smaller than that of N-G/FePc/Nafion/PLL ITO electrode because of the improved reactivity and electrocatalytic of N-G. While for N-G/Nafion/PLL ITO electrode, the peak current density was remarkably larger than that at the FePc/Nafion/PLL ITO electrode, GO/FePc/Nafion/PLL ITO electrode and G/FePc/Nafion/PLL ITO electrode meaning that the electrocatalytic activity to the oxidation of NO could be effectively enhanced by N-G. The high porosity and large surface area of N-G facilitated the adsorption of NO molecules. As shown in Figure 3B (purple curve), the N-G/FePc/Nafion/PLL ITO electrode exhibits an appreciable enhancement in electrocatalytic oxidation current density and well-defined peaks with a separation of anodic peak potentials smaller than that of the other modified electrodes, indicating that N-G decorated with FePc presents a synergistic effect that could greatly improve the electrocatalytic ability for the oxidation of NO.[28,39] As a highly conductive bridge, N-G facilitated rapid transport of electrons between the phthalocyanine and the electrode.[23,41]

Kinetics study of N-G/FePc/Nafion/PLL ITO electrode toward NO response. In order to obtain further information on the catalytic mechanism of the oxidation process for NO at the N-G/FePc/Nafion/PLL ITO electrode, the effect of scan rate was studied by CV. Figure 4 shows that the plot of anodic peak current densities increase linearly with increasing scan rates from 25 to 600 mV s^{-1} with a correlation coefficient of 0.9955, which suggests a surface-controlled kinetic process on the modified electrode surface.[42,43] Meanwhile, the peak potential exhibited a slightly positive shift with the increase of scan rate and the corresponding cathodic peak did not appear indicating the irreversibility of the NO electrocatalytic oxidation process.[44]

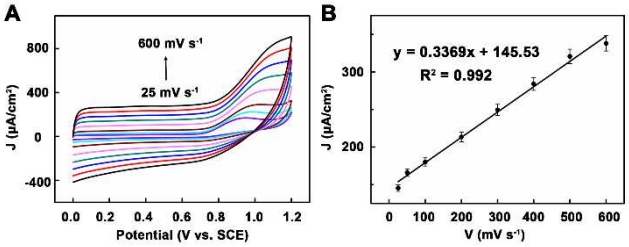

Figure 4. (A) Cyclic voltammograms of 216 μM NO in 0.01 M PBS on N-G/FePc/Nafion/PLL ITO electrode, at different scan rates (25, 50, 100, 200, 300, 400, 500 and 600 mV s^{-1}). (B) Linear variation of peak currents vs. scan rates related to the oxidation of NO (the CV baseline/charging current have been subtracted).

The reaction scheme for NO electrocatalytic oxidation on metallophthalocyanines was studied by Bedioui *et al*.[20] The mechanism of NO oxidation on N-G/FePc/Nafion/PLL ITO electrode could be proposed that NO was firstly adsorbed on FePc and increased the electron density partially, followed by transferring an electron to form NO^+:[45]

$$\text{Pc-Fe(II)} \rightleftharpoons [\text{Pc-Fe(III)}]^+ + e^- \quad [1]$$

$$[\text{Pc-Fe(III)}]^+ + \text{NO} \rightleftharpoons [\text{PcFe(III)}^{\delta-}\text{-(NO)}^{\delta+}]^+ \quad [2]$$

$$[\text{PcFe(III)}^{\delta-}\text{-(NO)}^{\delta+}]^+ \xrightarrow{rds} [\text{PcFe(III)}]^+ + \text{NO}^+ + e^- \quad [3]$$

Figure S2A presents LSV analysis of the N-G/FePc modified rotating disk electrode. The Tafel plot gives almost linear correlations with slope of *ca.* 0.12 V/decade (Figure S2B), which indicates that the transfer of the first electron (step 3) is rate determining (with a near-symmetrical energy barrier).[20] After that NO^+ could further react with water towards nitrite (NO^{2-}) through a homogeneous reaction. In some case, the formed electrochemically active NO^{2-} was converted to nitrate (NO^{3-}) by a two-electron process:[46,47]

$$NO^+ + H_2O \rightarrow HNO_2 + H^+$$

$$HNO_2 \rightleftharpoons NO_2^- + H^+$$

$$NO_2^- + H_2O \rightarrow NO_3^- + 2H^+ + 2e^-$$

Quantitative detection of NO at N-G/FePc/Nafion/PLL ITO electrode. To investigate the response character and linear range of the optimized biosensor, the amperometric response of N-G/FePc/Nafion/PLL ITO electrode at an applied potential of 0.9 V (vs. SCE) was recorded to successive addition of increased concentrations of NO into PBS (0.01 M, pH 7.4) with a continuous stirring. As shown in Figure 5A, the oxidation current densities of NO occurr instantaneously on the addition of an aliquot of NO and reach 90% of the steady-state response current in less than 4 s, which was shorter than the physiological lifetime (~5 s) of NO.[35] Such a rapid response might be attributed to the superb catalytic activity and promoted electron transfer afforded by the combination of N-G and FePc as well as the sufficient contact area of ITO electrode with unlimited mass diffusion. The inset of Figure 5A describes the successive addition with lower concentration of 180 nM and 720 nM NO in which a stepwise growth of the oxidation current density can also be observed. Figure 5B displays the calibration plot of the sensor. The amperometric current response was increased linearly with increasing NO concentrations in the range of 1.8×10^{-7}– 4×10^{-4} mol L^{-1} with a linear regression equation of J ($\mu A/cm^2$) = 0.085 + 0.208C (μM) (R^2 = 0.994). The sensitivity of the NO sensor obtained from the slope was 0.21 $\mu A\ \mu M^{-1}\ cm^{-2}$ and the detection limit was 180 nmol L^{-1} at a signal-to noise ratio of 3. The current N-G/FePc/Nafion/PLL ITO sensor demonstrated a wider linear range and relatively low detection limit compared with the previous electrochemical sensors of NO (Table S1, ESI†).

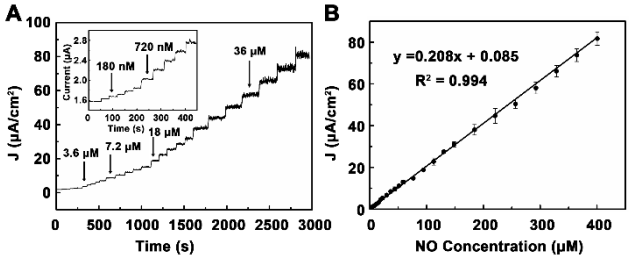

Figure 5. (A) Amperometric response of the N-G/FePc/Nafion/PLL ITO electrode to the successive addition of different concentration of NO in PBS at an applied potential of 0.9 V. Inset: amplified response of the modified electrode to lower concentrations of NO. (B) The calibration curve of the N-G/FePc/Nafion/PLL ITO electrode to NO.

Selectivity of the NO electrochemical sensor to common biological interfering species is important for practical applications. Amperometric responses of N-G/FePc/Nafion/PLL ITO electrode were carried out to investigate the effect of KCl, Na_2SO_4, $NaNO_2$, glucose, $Ca(NO_3)_2$ (the added concentration at 36 μM was higher than their physiological levels) towards the detection of NO in a homogeneously stirring PBS at an applied potential of 0.9 V (Figure 6). Figure 6A clearly indicates that the sensor has a remarkably larger current response for NO (36 μM) than that resulting from these interfering species (signal change less than 8.0%). Moreover, the small influences of nitrite (NO_2^-) ($NaNO_2$ was used as the precursor to produce NO) at the same concentration (signal changes<10%) could be contributed from the negatively-charged Nafion film acting as a barrier to repel the negatively charged nitrite due to the electrostatic repulsion while allowing the free penetration of neutral NO molecules (Figure 6B).[48] The satisfactory selectivity of the sensor matrix also came from high catalytic activity of N-G/FePc nanocomposite specifically toward NO oxidation.

Five N-G/FePc/Nafion/PLL ITO electrodes were fabricated under the same condition and showed an acceptable reproducibility with a relative standard deviation (RSD) of 4.3% for the amperometric response to 18 μM NO. The RSD of the current response to 18 μM NO was 5.2% for 5 successive measurements. In addition, the long-term stability of the sensor to NO was also investigated. As shown in the Figure S3, it kept nearly similar responses (96%) with negligible drop in the current signal over 10 days and the current still retained about 90% of its initial response value after the N-G/FePc/Nafion/PLL ITO electrode was stored at 4 °C for 20 days.

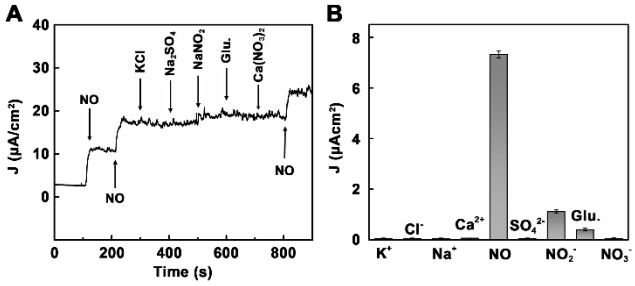

Figure 6. (A) Amperometric responses to 36 μM NO, KCl, Na_2SO_4, $NaNO_2$, glucose and $Ca(NO_3)_2$. (B) The selective profile.

Real-time measurement of nitric oxide molecules released from living cells. Human umbilical vein endothelial cells (HUVECs) are widely used as the cell model of vascular endothelial cell when research on the vasoactive substances secreted by endothelial cell including nitric oxide. Here, the N-G/FePc/ Nafion/PLL ITO sensor was used to real-time and in situ detect NO molecules released from living HUVECs in response to L-Arg stimulation. The direct contact between HUVECs and the modified ITO electrode bring high efficient capture of NO molecules after injection of L-Arg which is a substrate for nitric oxide synthase (NOS) in biological systems.[48] Nω-nitro-L-arginine methyl ester hydrochloride (L-NAME), a competitive inhibitor of NOS was used as a model drug to inhibit the generation of nitric oxide.

After seeding on the N-G/FePc/Nafion/PLL ITO electrode and the bare ITO electrode to adhere for 18 h when the cell growth rate became slow,[49] the adherent cells were observed by inverted fluorescent microscopy. As displayed in Figure

7A, HUVECs cultured on N-G/FePc/Nafion/PLL ITO electrode (Figure 7A, right) have a better cell morphology than those cultured on the bare ITO (Figure 7A, left), suggesting that such a modified electrode is a biocompatible platform for cell's attachment. Then the N-G/FePc/Nafion/PLL ITO electrode was applied to detect real time NO generation from HUVECs by measuring the amperometric response at a constant potential of 0.9 V vs. SCE.

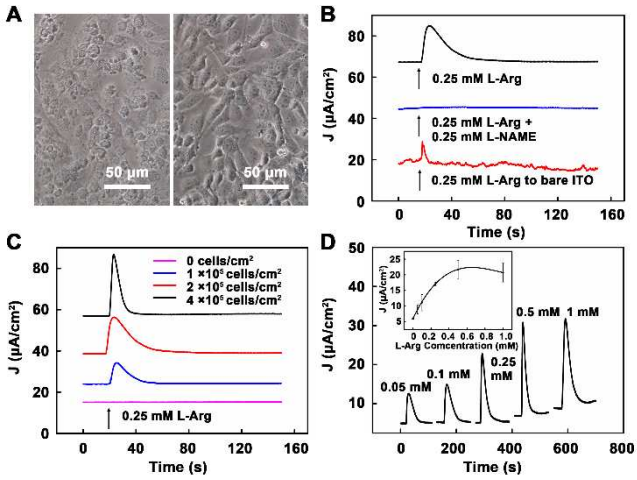

Figure 7. (A) Microscope photographs of HUVECs cultured on the bare ITO electrode (left) and the N-G/FePc/Nafion/PLL ITO electrode (right) after seeding for 18 h. (B) Real-time monitoring of NO released from HUVECs cultured on the N-G/FePc/Nafion/PLL ITO electrode (black and blue line) and the bare ITO electrode (red line) at different conditions. The drug was added at the time indicated by the arrow. (C) Real-time monitoring of NO released from HUVECs stimulated by 0.25 mM L-Arg in cell culture medium with controlled cell density. (D) Real-time monitoring of NO released from HUVECs stimulated by different amount of L-Arg. Inset: the response curve of the HUVECs cultured on the N-G/FePc/Nafion/PLL ITO electrode to different amount of L-Arg.

When 0.25 mM L-Arg was injected towards the cell surfaces, an obvious increase in current density was observed in Figure 7B (black line), in which the upward arrows indicated the injecting time of the drug. During 5-15 s after stimulation of L-Arg, the current increased to a maximum value (17.8 μA/cm^2) that was equivalent to instantaneous increase of NO concentration up to approximately 85.3 μM. Subsequently, the current decreased gradually to the baseline within 200 s. Under the same conditions, the amperometric response of the HUVECs on bare ITO electrode showed a small but sharp peak with large noise baseline (Figure 7B, red line), which could be attributed to the poor cell growth on bare ITO electrode and its relatively weak electro-catalytic capability compared to N-G/FePc/Nafion/PLL ITO electrode. As a control experiment, when a mixture of 0.25 mM L-Arg and 0.25 mM L-NAME was injected, the peak current showed obvious decrease by 98% under such circumstances (Figure 7B, blue line), which should be attributed to the specific inhibiting behavior of L-NAME towards NO release. This result also indicated that the change of the measured current was due to the oxidation of NO released from HUVECs.

Moreover, amperometric responses of the NO sensor to HUVECs with different cell densities are investigated as shown in Figure 7C. The N-G/FePc/Nafion/PLL ITO electrode don't exhibit any response to blank ITO without HUVECs (pink line), indicating that the response was not due to the addition of L-Arg. After cell densities in this ITO electrode are controlled as 1 × 10^5 cells/cm^2 (blue line), 2 × 10^5 cells/cm^2 (red line) and 4 × 10^5 cells/cm^2 (black line), the current responses generated from HUVECs with stimulation of 0.25 mM L-Arg can be measured and equivalent to approximately 46.0 μM, 85.3 μM and 142.9 μM NO release, respectively. Obviously, the NO concentrations increased with the cell density in nearly equal proportions. The current responses caused by adding 0.25 mM L-Arg to HUVECs with 2 × 10^5 cells/cm^2 are about 1.85 times than that of 1 × 10^5 cells/cm^2 cell density. These results clearly demonstrate that the N-G/FePc/Nafion/PLL ITO electrodes are capable of the real-time monitoring of extracellular NO generated from HUVECs at different cell densities.

In order to further investigate the performance of the N-G/FePc/Nafion/PLL ITO electrode toward different concentrations of L-Arg, successive injection of L-Arg from 0.05 mM to 1 mM towards cell surfaces was carried out in PBS (Figure 7D). The NO releases from HUVECs are also drug-concentration dependent, where the current values are 9.6 and 17.8 μA/cm^2 at 0.1 and 0.25 mM L-Arg stimulation, respectively. The current response exhibited a similar varying trend when higher dose of L-Arg (0.5 mM) was injected into the same electrode surface, while the peak current intensity (23.7 μA/cm^2) was less than two times than that of 0.25 mM L-Arg stimulation. And then the current response was no longer increase with the increasing L-Arg dose. The inset of Figure 7D displayed the response curve of the HUVECs cultured on the N-G/FePc/Nafion/PLL ITO electrode to different amount of L-Arg. This result showed that the process of drug trigger was not fully proportional to the concentrations of the stimulus, perhaps because of the complicated biosynthetic mechanism of NO in HUVECs. Successive addition of the same concentration of L-Arg to HUVECs showed the NO sensor remained 80% of its initial response after cell stimulated and sensor renewal 3 times (Figure S4), indicating a satisfying repeatability when the N-G/FePc/Nafion/PLL ITO electrode was used to real-time monitoring NO in complex biological systems.

CONCLUSION

In brief, we have developed a high-performance N-G/FePc/Nafion/PLL ITO electrochemical sensing platform for real-time monitoring of NO released from living cells. The FePc was well-distributed on the surface of N-G via non-covalently functionalization which induced more active sites for the catalytic redox action. Due to the remarkable synergistic effect of N-G and FePc nanocomposite layer, the biosensor displayed superior conductivity and excellent electrocatalytic activity toward NO oxidation. The current response of N-G/FePc/Nafion/PLL ITO electrode was measured in a broad concentration range of 0.18–400 μM, where the electrode exhibited a linear response with the LOD of 0.18 μM. This is the first report of a cell growth N-G/FePc/Nafion/PLL ITO sensing interface which allows seamless signal transduction from adhesive HUVECs to the sensor itself. This protocol not only offers a convenient route to fabricate N-G/FePc nanocompo-

site with specific properties, but also establishes a potential platform for highly biocompatible real-time monitoring of NO and other biomarkers in clinical diagnostics.

ASSOCIATED CONTENT

AUTHOR INFORMATION

Corresponding Author

* E-mail: bcye@ecust.edu.cn

* E-mail: bhliu@fudan.edu.cn. Fax: +86-21-65641740

ORCID

Bang-Ce Ye: 0000-0002-5555-5359

Baohong Liu: 0000-0002-0660-8610

Notes

The authors declare no competing financial interest.

ACKNOWLEDGMENT

This work was supported by the National Natural Science Foundation of China (Grant No. 21705047 and 21335003), the Chinese Post-Doctoral Fund (Grant No. 2017M621380) and the Fundamental Research Funds for the Central Universities (Grant No. 222201814030).

REFERENCES

(1) Palmer, R. M. J.; Ferrige, A. G.; Moncada, S. Nitric Oxide Release Accounts for the Biological Activity of Endothelium-Derived Relaxing Factor. *Nature* **1987**, *327*, 524-526.

(2) Cha, W.; Tung, Y.-C.; Meyerhoff, M. E.; Takayama, S. Patterned Electrode-Based Amperometric Gas Sensor for Direct Nitric Oxide Detection within Microfluidic Devices. *Anal. Chem.* **2010**, *82*, 3300-3305.

(3) Hunter, R. A.; Privett, B. J.; Henley, W. H.; Breed, E. R.; Liang, Z.; Mittal, R.; Yoseph, B. P.; McDunn, J. E.; Burd, E. M.; Coopersmith, C. M.; Ramsey, J. M.; Schoenfisch, M. H. Microfluidic Amperometric Sensor for Analysis of Nitric Oxide in Whole Blood. *Anal. Chem.* **2013**, *85*, 6066-6072.

(4) Hunter, R. A.; Storm, W. L.; Coneski, P. N.; Schoenfisch, M. H. Inaccuracies of Nitric Oxide Measurement Methods in Biological Media. *Anal. Chem.* **2013**, *85*, 1957-1963.

(5) Griveau, S.; Bedioui, F. Overview of Significant Examples of Electrochemical Sensor Arrays Designed for Detection of Nitric Oxide and Relevant Species in a Biological Environment. *Anal. Bioanal. Chem.* **2013**, *405*, 3475-3488.

(6) Evig, C. B.; Kelley, E. E.; Weydert, C. J.; Chu, Y.; Buettner, G. R.; Patrick Burns, C. Endogenous Production and Exogenous Exposure to Nitric Oxide Augment Doxorubicin Cytotoxicity for Breast Cancer Cells but not Cardiac Myoblasts. *Nitric Oxide* **2004**, *10*, 119-129.

(7) Ye, X.; Rubakhin, S. S.; Sweedler, J. V. Detection of Nitric Oxide in Single Cells. *Analyst* **2008**, *133*, 423-433.

(8) Jo, A.; Do, H.; Jhon, G.-J.; Suh, M.; Lee, Y. Electrochemical Nanosensor for Real-Time Direct Imaging of Nitric Oxide in Living Brain. *Anal. Chem.* **2011**, *83*, 8314-8319.

(9) Bedioui, F.; Griveau, S. Electrochemical Detection of Nitric Oxide: Assessement of Twenty Years of Strategies. *Electroanalysis* **2013**, *25*, 587-600.

(10) Peng, Y.; Ji, Y.; Zheng, D.; Hu, S. In Situ Monitoring of Nitric Oxide Release from Rat Kidney at Poly(eosin b)-Ionic Liquid Composite-based Electrochemical Sensors. *Sens. Actuators, B* **2009**, *137*, 656-661.

(11) Nyokong, T.; Vilakazi, S. Phthalocyanines and Related Complexes as Electrocatalysts for the Detection of Nitric Oxide. *Talanta* **2003**, *61*, 27-35.

(12) Xu, T.; Scafa, N.; Xu, L.-P.; Su, L.; Li, C.; Zhou, S.; Liu, Y.; Zhang, X. Electrochemical Sensors for Nitric Oxide Detection in Biological Applications. *Electroanalysis* **2014**, *26*, 449-468.

(13) Liu, Y.-L.; Jin, Z.-H.; Liu, Y.-H.; Hu, X.-B.; Qin, Y.; Xu, J.-Q.; Fan, C.-F.; Huang, W.-H. Stretchable Electrochemical Sensor for Real-Time Monitoring of Cells and Tissues. *Angew. Chem., Int. Ed.* **2016**, *55*, 4537-4541.

(14) Kim, M.-Y.; Naveen, M. H.; Gurudatt, N. G.; Shim, Y.-B. Detection of Nitric Oxide from Living Cells Using Polymeric Zinc Organic Framework-Derived Zinc Oxide Composite with Conducting Polymer. *Small* **2017**, *13*, 1700502-n/a.

(15) Moon, J.; Ha, Y.; Kim, M.; Sim, J.; Lee, Y.; Suh, M. Dual Electrochemical Microsensor for Real-Time Simultaneous Monitoring of Nitric Oxide and Potassium Ion Changes in a Rat Brain during Spontaneous Neocortical Epileptic Seizure. *Anal. Chem.* **2016**, *88*, 8942-8948.

(16) Elliott, J.; Duay, J.; Simoska, O.; Shear, J. B.; Stevenson, K. J. Gold Nanoparticle Modified Transparent Carbon Ultramicroelectrode Arrays for the Selective and Sensitive Electroanalytical Detection of Nitric Oxide. *Anal. Chem.* **2017**, *89*, 1267-1274.

(17) Obirai, J. C.; Nyokong, T. Thiol Oxidation at 2-Mercaptopyrimidine-Appended Cobalt Phthalocyanine Modified Glassy Carbon Electrodes. *J. Electroanal. Chem.* **2007**, *600*, 251-256.

(18) Pereira-Rodrigues, N.; Cofré, R.; Zagal, J. H.; Bedioui, F. Electrocatalytic Activity of Cobalt Phthalocyanine CoPc Adsorbed on a Graphite Electrode for the Oxidation of Reduced L-glutathione (GSH) and the Reduction of Its Disulfide (GSSG) at Physiological pH. *Bioelectrochem.* **2007**, *70*, 147-154.

(19) Zagal, J. H.; Griveau, S.; Silva, J. F.; Nyokong, T.; Bedioui, F. Metallophthalocyanine-Based Molecular Materials as Catalysts for Electrochemical Reactions. *Coord. Chem. Rev.* **2010**, *254*, 2755-2791.

(20) Caro, C. A.; Zagal, J. H.; Bedioui, F. Electrocatalytic Activity of Substituted Metallophthalocyanines Adsorbed on Vitreous Carbon Electrode for Nitric Oxide Oxidation. *J. Electrochem. Soc.* **2003**, *150*, E95-E103.

(21) Francisco Silva, J.; Griveau, S.; Richard, C.; Zagal, J. H.; Bedioui, F. Glassy Carbon Electrodes Modified with Single Walled Carbon Nanotubes and Cobalt Phthalocyanine and Nickel Tetrasulfonated Phthalocyanine: Highly Stable New Hybrids with Enhanced Electrocatalytic Performances. *Electrochem. Commun.* **2007**, *9*, 1629-1634.

(22) Vilakazi, S. L.; Nyokong, T. Voltammetric Determination of Nitric Oxide on Cobalt Phthalocyanine Modified Microelectrodes. *J. Electroanal. Chem.* **2001**, *512*, 56-63.

(23) Liu, Y.-L.; Wang, X.-Y.; Xu, J.-Q.; Xiao, C.; Liu, Y.-H.; Zhang, X.-W.; Liu, J.-T.; Huang, W.-H. Functionalized Graphene-Based Biomimetic Microsensor Interfacing with Living Cells to Sensitively Monitor Nitric Oxide Release. *Chem. Sci.* **2015**, *6*, 1853-1858.

(24) Sheng, Z.-H.; Shao, L.; Chen, J.-J.; Bao, W.-J.; Wang, F.-B.; Xia, X.-H. Catalyst-Free Synthesis of Nitrogen-Doped Graphene via Thermal Annealing Graphite Oxide with Melamine and Its Excellent Electrocatalysis. *ACS Nano* **2011**, *5*, 4350-4358.

(25) Qu, L.; Liu, Y.; Baek, J.-B.; Dai, L. Nitrogen-Doped Graphene as Efficient Metal-Free Electrocatalyst for Oxygen Reduction in Fuel Cells. *ACS Nano* **2010**, *4*, 1321-1326.

(26) Wang, Y.; Shao, Y.; Matson, D. W.; Li, J.; Lin, Y. Nitrogen-Doped Graphene and Its Application in Electrochemical Biosensing. *ACS Nano* **2010**, *4*, 1790-1798.

(27) Tu, W.; Lei, J.; Jian, G.; Hu, Z.; Ju, H. Noncovalent Assembly of Picket-Fence Porphyrins on Nitrogen-Doped Carbon Nanotubes for Highly Efficient Catalysis and Biosensing. *Chem. - Eur. J.* **2010**, *16*, 4120-4126.

(28) Xu, H.; Xiao, J.; Liu, B.; Griveau, S.; Bedioui, F. Enhanced Electrochemical Sensing of Thiols Based on Cobalt Phthalocyanine Immobilized on Nitrogen-Doped Graphene. *Biosens. Bioelectron.* **2015**, *66*, 438-444.

(29) Siswana, M. P.; Ozoemena, K. I.; Nyokong, T. Electrocatalysis of Asulam on Cobalt Phthalocyanine Modified Multi-Walled Carbon

Nanotubes Immobilized on a Basal Plane Pyrolytic Graphite Electrode. *Electrochim. Acta* **2006**, *52*, 114-122.
(30) Xie, H.; Li, Y.-T.; Lei, Y.-M.; Liu, Y.-L.; Xiao, M.-M.; Gao, C.; Pang, D.-W.; Huang, W.-H.; Zhang, Z.-Y.; Zhang, G.-J. Real-Time Monitoring of Nitric Oxide at Single-Cell Level with Porphyrin-Functionalized Graphene Field-Effect Transistor Biosensor. *Anal. Chem.* **2016**, *88*, 11115-11122.
(31) Cao, J.-T.; Hao, X.-Y.; Zhu, Y.-D.; Sun, K.; Zhu, J.-J. Microfluidic Platform for the Evaluation of Multi-Glycan Expressions on Living Cells using Electrochemical Impedance Spectroscopy and Optical Microscope. *Anal. Chem.***2012**, *84*, 6775-6782.
(32) Sun, X.; Gillis, K. D. On-Chip Amperometric Measurement of Quantal Catecholamine Release Using Transparent Indium Tin Oxide Electrodes. *Anal. Chem.* **2006**, *78*, 2521-2525.
(33) Li, C. M.; Zang, J.; Zhan, D.; Chen, W.; Sun, C. Q.; Teo, A. L.; Chua, Y. T.; Lee, V. S.; Moochhala, S. M. Electrochemical Detection of Nitric Oxide on a SWCNT/RTIL Composite Gel Microelectrode. *Electroanalysis* **2006**, *18*, 713-718.
(34) Mesároš, Š.; Grunfeld, S.; Mesárošová, A.; Bustin, D.; Malinski, T. Determination of Nitric Oxide Saturated (stock) Solution by Chronoamperometry on a Porphyrine Microelectrode. *Anal. Chimi. Acta* **1997**, *339*, 265-270.
(35) Ting, S. L.; Guo, C. X.; Leong, K. C.; Kim, D.-H.; Li, C. M.; Chen, P. Gold Nanoparticles Decorated Reduced Graphene Oxide for Detecting the Presence and Cellular Release of Nitric Oxide. *Electrochim. Acta* **2013**, *111*, 441-446.
(36) Wang, Q.; Li, H.; Yang, J.-H.; Sun, Q.; Li, Q.; Yang, J. Iron Phthalocyanine-Graphene Donor-Acceptor Hybrids for Visible-Light-Assisted Degradation of Phenol in the Presence of H_2O_2. *Appl. Catal. B-Environ.* **2016**, *192*, 182-192.
(37) Yuan, G.; Zhang, G.; Zhou, Y.; Yang, F. Synergetic Adsorption and Catalytic Oxidation Performance Originating from Leafy Graphite Nanosheet Anchored Iron(II) Phthalocyanine Nanorods for Efficient Organic Dye Degradation. *RSC Adv.* **2015**, *5*, 26132-26140.
(38) Sheng, Z.-H.; Zheng, X.-Q.; Xu, J.-Y.; Bao, W.-J.; Wang, F.-B.; Xia, X.-H. Electrochemical Sensor Based on Nitrogen Doped Graphene: Simultaneous Determination of Ascorbic Acid, Dopamine and Uric Acid. *Biosens. Bioelectron.* **2012**, *34*, 125-131.
(39) Shanmugam, S.; Osaka, T. Efficient Electrocatalytic Oxygen Reduction over Metal Free-Nitrogen Doped Carbon Nanocapsules. *Chem. Commun.* **2011**, *47*, 4463-4465.
(40) Kannan, P.; John, S. A. Highly Sensitive Electrochemical Determination of Nitric Oxide Using Fused Spherical Gold Nanoparticles Modified ITO Electrode. *Electrochim. Acta* **2010**, *55*, 3497-3503.
(41) Xu, Y.; Zhao, L.; Bai, H.; Hong, W.; Li, C.; Shi, G. Chemically Converted Graphene Induced Molecular Flattening of 5,10,15,20-Tetrakis(1-methyl-4-pyridinio)porphyrin and Its Application for Optical Detection of Cadmium(II) Ions. *J. Am. Chem. Soc.* **2009**, *131*, 13490-13497.
(42) Cruz Moraes, F.; Cabral, M. F.; Machado, S. A. S.; Mascaro, L. H. Electrocatalytic Behavior of Glassy Carbon Electrodes Modified with Multiwalled Carbon Nanotubes and Cobalt Phthalocyanine for Selective Analysis of Dopamine in Presence of Ascorbic Acid. *Electroanalysis* **2008**, *20*, 851-857.
(43) Brown, A. P.; Anson, F. C. Cyclic and Differential Pulse Voltammetric Behavior of Reactants Confined to the Electrode Surface. *Anal. Chem.* **1977**, *49*, 1589-1595.
(44) Yan, Y.; Yao, P.; Mu, Q.; Wang, L.; Mu, J.; Li, X.; Kang, S.-Z. Electrochemical Behavior of Amino-Modified Multi-Walled Carbon Nanotubes Coordinated with Cobalt Porphyrin for the Oxidation of Nitric Oxide. *Appl. Surf. Sci.* **2011**, *258*, 58-63.
(45) Li, J.; Xie, J.; Gao, L.; Li, C. M. Au Nanoparticles–3D Graphene Hydrogel Nanocomposite To Boost Synergistically in Situ Detection Sensitivity toward Cell-Released Nitric Oxide. *ACS Appl. Mater. Interfaces* **2015**, *7*, 2726-2734.
(46) Liu, Y. M.; Punckt, C.; Pope, M. A.; Gelperin, A.; Aksay, I. A. Electrochemical Sensing of Nitric Oxide with Functionalized Graphene Electrodes. *ACS Appl. Mater. Interfaces* **2013**, *5*, 12624-12630.
(47) Ananthi, A.; Phani, K. L. Self-Assembly of Gold Nanoparticles on sulphide Functionalized Polydopamine in Application to Electrocatalytic Oxidation of Nitric Oxide. *J. Electroanal. Chem.* **2016**, *764*, 7-14.
(48) Dang, X.; Hu, C.; Wang, Y.; Hu, S. Gold Nanoparticle Film Grown on Quartz Fiber and Its Application as a Microsensor of Nitric Oxide. *Sens. Actuators, B* **2011**, *160*, 260-265.
(49) Guo, C. X.; Ng, S. R.; Khoo, S. Y.; Zheng, X.; Chen, P.; Li, C. M. RGD-Peptide Functionalized Graphene Biomimetic Live-Cell Sensor for Real-Time Detection of Nitric Oxide Molecules. *ACS Nano* **2012**, *6*, 6944-6951.

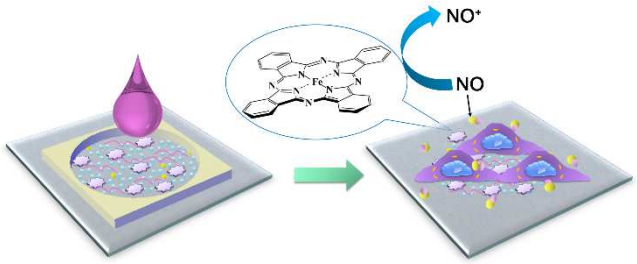

For TOC only